Blood First Edition Paper, prepublished online September 19, 2019; DOI 10.1182/blood.2019001705

American Society of Hematology
2021 L Street NW, Suite 900,
Washington, DC 20036
Phone: 202-776-0544 | Fax 202-776-0545
editorial@hematology.org

The architecture of the IgG anti-carbohydrate repertoire in primary antibody deficiencies (PADs)

Tracking no: BLD-2019-001705R1-FINALFILES

Peter Jandus (University Hospital of Geneva, Switzerland) Kayluz Frias Boligan (University of Bern,) David Smith (Emory University School of Medicine, United States) Elisabeth de Graauw (University of Bern, Switzerland) Bodo Grimbacher (Satellite Center Freiburg, Germany) Camilla Jandus (University of Bern, Switzerland) Mai Abdelhafez (Modern Science and Art University (MSA), Egypt) Alain Despont (University of Bern, Switzerland) Nicolai Bovin (Auckland University of Technology, New Zealand) Dagmar Simon (Inselspital, Switzerland) Robert Rieben (University of Bern, Switzerland) Hans-Uwe Simon (University of Bern, Switzerland) Richard Cummings (Harvard Medical School, United States) Stephan von Gunten (Institute of Pharmacology, University of Bern, Switzerland)

Abstract:
Immune system failure in primary antibody deficiencies (PADs) has been linked to recurrent infections, autoimmunity and cancer, yet clinical judgment is often based on the reactivity to a restricted panel of antigens. Previously, we demonstrated that the human repertoire of carbohydrate-specific IgG exhibits modular organization related to glycan epitope structure. The current study compares the glycan-specific IgG repertoires among different PAD entities. Distinct repertoire profiles with extensive qualitative glycan-recognition defects were observed, characterized by the common loss of Gala- and GalNAc-reactivity and disease-specific recognition of microbial, self-antigens and tumor-associated carbohydrate antigens. Antibody repertoire analysis may provide a useful tool to elucidate the dimension and clinical implications of the immune system failure in individual patients.

Conflict of interest: No COI declared

COI notes:

Preprint server: No;

Author contributions and disclosures: S.V.G. and P.J. designed the study. K.F.B., P.J. and S.V.G. wrote the manuscript. K.F.B. and S.V.G. analyzed the data. Glycan array experiments at the CFG were conducted under supervision of D.F.S. and R.D.C. Database searches and computational analysis of the data set was performed by K.F.B. Patient sample collection, classification and preparation were done by B. G., C.J. and P.J. Experimental work was done by K.F.B., E.D.G., M.A., A.D. under supervision by D.S., H.U.S., R.R. and S.V.G. Glycan synthesis was supervised by N.B. All authors had full access to the data, helped draft the report or critically revised the draft, contributed to data interpretation, reviewed and approved the final version of the report.

Non-author contributions and disclosures: No;

Agreement to Share Publication-Related Data and Data Sharing Statement: emails to the corresponding author

Clinical trial registration information (if any):

The architecture of the IgG anti-carbohydrate repertoire in primary antibody deficiencies (PADs)

Running tittle: Carbohydrate-specific IgG repertoire in PAD

Author list: Peter Jandus[1†], Kayluz Frias Boligan[2†], David F. Smith[3], Elisabeth de Graauw[2], Bodo Grimbacher[4-7], Camilla Jandus[2,8,9], Mai M. Abdelhafez[10], Alain Despont[10], Nicolai Bovin[11,12], Dagmar Simon[13], Robert Rieben[10], Hans-Uwe Simon[2,14], Richard D. Cummings[3, 15], Stephan von Gunten[2]

[1]Division of Clinical Immunology and Allergy, Department of Internal Medicine, University Hospital and Faculty of Medicine, Geneva, Switzerland

[2]Institute of Pharmacology, University of Bern, Bern, Switzerland

[3]Emory Comprehensive Glycomics Core, Department of Biochemistry, Emory University School of Medicine, Atlanta, GA, USA

[4]Institute for Immunodeficiency, Center for Chronic Immunodeficiency (CCI), Medical Center, Faculty of Medicine, Albert-Ludwigs-University of Freiburg, Germany

[5]DZIF – German Center for Infection Research, Satellite Center Freiburg, Germany

[6]CIBSS – Centre for Integrative Biological Signalling Studies, Albert-Ludwigs University, Freiburg, Germany

[7]RESIST – Cluster of Excellence 2155 to Hanover Medical School, Satellite Center Freiburg, Germany

[8]Translational cytokine secreting lymphocyte group, Department of Oncology UNIL CHUV, University of Lausanne, Lausanne, Switzerland

[9]Ludwig Institute for Cancer Research, University of Lausanne, Lausanne, Switzerland

[10]Department for BioMedical Research (DBMR), University of Bern, Bern, Switzerland

[11]Shemyakin-Ovchinnikov Institute of Bioorganic Chemistry Russian Academy of Science, Moscow, Russian Federation

[12]Auckland University of Technology, Auckland, New Zealand

[13]Department of Dermatology, Inselspital, Bern University Hospital, University of Bern, Bern, Switzerland

[14]Department of Clinical Immunology and Allergology, Sechenov University, Moscow, Russia.

[15]Department of Surgery, Beth Israel Deaconess Medical Center, Harvard Medical School, Boston, Massachusetts, USA

Corresponding author: Stephan von Gunten, University of Bern, 3012 Bern, Switzerland. Phone: 41-31-632-32-98; Fax: 41-31-632-49-94. E-mail: stephan.vongunten@pki.unibe.ch

KEY WORDS: Primary immunodeficiency diseases (PID), primary antibody deficiencies (PAD), common variable immunodeficiency disorders (CVID), glycan array, xenotransplantation

Article length: 3’818 words

KEY POINTS: Repertoire analysis by microarray technology constitutes a powerful tool to evaluate immune system failure in PADs.

ABSTRACT

Immune system failure in primary antibody deficiencies (PADs) has been linked to recurrent infections, autoimmunity and cancer, yet clinical judgment is often based on the reactivity to a restricted panel of antigens. Previously, we demonstrated that the human repertoire of carbohydrate-specific IgG exhibits modular organization related to glycan epitope structure. The current study compares the glycan-specific IgG repertoires among different PAD entities. Distinct repertoire profiles with extensive qualitative glycan-recognition defects were observed, characterized by the common loss of Galα- and GalNAc-reactivity and disease-specific recognition of microbial, self-antigens and tumor-associated carbohydrate antigens. Antibody repertoire analysis may provide a useful tool to elucidate the dimension and clinical implications of the immune system failure in individual patients.

Abstract length: 114 words

INTRODUCTION

Inadequate humoral responses to carbohydrate-structures represent a common feature of primary antibody deficiencies (PADs), despite the pathogenetic heterogeneity of these disorders, involving monogenetic, polygenetic and still unexplained defects[1,2]. These disorders are associated with a plethora of clinical sequelae including severe and recurrent infections, microbial dysbiosis, autoimmunity, allergy, granulomatous disease and malignancy[1,3,4].

The surface of all living cells is glycosylated, whereby the composition varies between cell type[5], individuals, or species[6]. The prominent exposure of carbohydrate-structures (glycans) on the surface of cells or bacterial capsules, renders them accessible to antibodies, which facilitates the detection and elimination of pathogens or aberrant cells, but also leads to adverse reaction in transfusion/transplantation procedures (blood groups antigens), or to the acute rejection of xenografts (e.g. Gal-α structures). Due to altered expression of biosynthetic enzymes, such as glycosyltransferases or glycosidases, the glycome of cells is often changed under pathological conditions, including cancer[7]. While tumor-associated carbohydrates (TACAs) are exploited as diagnostic markers[8], there is also evidence for naturally-occurring antibodies to TACAs in healthy individuals[9].

Insufficient responses to glycan-based vaccines or low titers of isohemagglutinins, antibodies to polysaccharide blood group antigens, are characteristic and diagnostic features of common variable immunodeficiency (CVID), the most frequent symptomatic antibody deficiency diagnosed in adulthood[10,11]. Patients with specific antibody deficiency (SPAD) exhibit poor responses to structural or capsular polysaccharides of bacteria (e.g. *S. pneumoniae, H. influenzae*), despite the presence of normal serum concentrations of IgG, IgM and IgA[12]. Antibodies from

different IgG subclasses are known to contain different specificities for glycan-structures[9,13], which may explain the predisposition of certain patients with IgG subclass deficiency (IgGSD) to infections with encapsulated bacteria[12]. However, current knowledge on the failure to raise adequate levels of glycan-specific antibodies in PAD is mainly based on experience with specific bacterial antigens.

The clinical assessment of PADs by diagnostic vaccination (e.g. pneumococcal vaccines, *S. typhi* Vi vaccine[14]) or the measurement of pre-existing antibody titers (e.g. isohemagglutinins) relies on a restricted number of glycan epitopes, thus providing only a narrow perspective of the actual dimensions of the immunodeficiency. Further disadvantages of diagnostic vaccination include diagnostic delay, laboratory-to-laboratory variation, serotype-specific responses, age differences in antibody responses, or the challenging interpretation of pre-immunization versus post-immunization specific antibody levels in patients not receiving IgG replacement therapy[10,11,15-18]. The broader assessment of glycan-specific antibodies in patients may better reflect the immune defect and also facilitate treatment decisions, such as regarding life-long IgG replacement therapy.

Glycan array technology allows the high-throughput analysis of specific antibody responses to carbohydrate antigens[19-21]. In a previous study using glycan array version 5.1 of The Consortium for Functional Glycomics (CFG) to decipher the IgG repertoire of healthy individuals we found that classes of glycans were recognized with different intensity, depending on the terminal carbohydrate-moiety[9]. Here, we employed glycan array technology to investigate the IgG antibody repertoire of PAD patients in terms of clinically relevant carbohydrate epitopes, including microbial glycans, self- or xenoantigens, and TACAs.

MATERIALS AND METHODS

Study design

This non-randomized study was designed to investigate the human IgG anti-carbohydrate repertoire, in healthy and disease conditions, using glycan array technology combined with a computational system level approach. To this end, sera or purified IgG from healthy individuals or patients, as well as control antibodies were screened on microarrays by the Consortium for Functional Glycomics (CFG) or the US National Center for Functional Glycomics (NCFG).

Patient samples

Human blood was collected from healthy individuals (HD) or patients upon informed and written consent in accordance with the Declaration of Helsinki. All experimental protocols were approved by the local institutional and/or licensing committees (KEK-BE: 148/10 and KEK No. 224/01). Therapeutic naïve patients followed at the University Hospital of Bern from January 2005 to December 2011 were retrospectively identified. Additional sera of therapeutic naïve patients without IgG replacement therapy were provided from B.G. CVID was defined in accordance with the criteria of the Pan-American Group for Immunodeficiency and the European Society for Immunodeficiency[22]. Inclusion criteria for IgGSD were a normal total IgG concentration with a significant decrease (more than two standard deviations below the mean for the age) in the serum concentrations of one or more IgG subclasses[23] with recurrent episodes of infection. Symptomatic hypogammaglobulinemia (HGG) was defined with decreased total IgG concentration, but not fulfilling criteria for CVID with respect to a reduction of two immunoglobulin isotypes and/or reduced response to vaccination. For diagnostic vaccination the pneumococcal polysaccharide vaccine

(PPV) Pneumovax-23 (MSD, Lucerne, Switzerland) was used in patients with IgG levels at or higher than 4 g/L. Levels of pneumococcal capsular polysaccharide (PCP) IgG > 50 mg/L and for PCP IgG2 > 40 mg/L were considered as normal. A sufficient PPV vaccination response was defined as PCP titers above these levels and/or PCP IgG and IgG2 levels above 100 mg/L and/or a 4-fold increase of post-vaccination PCP IgG and PCP IgG2 titers as detected 4 to 6 weeks after vaccination. SPAD was diagnosed in patients with normal total immunoglobulin and IgG subclass concentrations but impaired pneumococcal polysaccharide vaccine (PPV) response. The characteristics of the different groups are summarized in Table S1. Patients were not stratified for specific infections. The sera from these patients were individually screened in the NCFGv2 glycan array or pooled in the indicated groups and screened in the CFG glycan array. IgG purification was performed by affinity chromatography in Ab SpinTrap columns (GE Healthcare). Pooled sera from patients and healthy donors were directly applied to the columns and the purification procedures performed according to manufacturer instructions. The control IgG preparation (IgG control mix) was prepared by mixing two monoclonal human myeloma proteins, IgG1λ (67%) and IgG2κ (33%), purchased from Sigma-Aldrich. This process resulted in a κ/λ ratio of 0.5, which is well within the range found in normal serum (0.26 to 1.65). The concentration of IgG in the different samples was determined using a Behring Turbitimer instrument (Dade Behring). The quality of the isolated antibodies was checked by SDS-PAGE under reducing and non-reducing conditions (Figure S1).

Glycan array analysis

The glycan microarrays from the CFG (http://www.functionalglycomics.org/static/consortium/resources/resourcecoreh8.shtm

l) were prepared from amine functionalized glycan structures covalently coupled in microarrays to N-hydroxysuccinimide-derivatized microscope slides as previously described[24]. On NCFG array version 2 (NCFGv2) carbohydrates were conjugated with the fluorescent linker AEAB, by reductive amination with sodium cyanoborohydrate to form glycan-AEABs (GAEABs). For both arrays, the human sera or purified IgG or IgG control mix, were identically processed and screened at 180μg/ml using a secondary biotinylated anti-human IgG mAb (clone HP-6043) at 5 μg/ml followed by Alexa633-coupled streptavidin[9]. A positive streptavidin control was used. Sample preparation and analysis was performed as indicated on the CFG website (www.functionalglycomics.org). To determine the specific binding to selected glycans, the antibody binding ratio (ABR) was calculated. The computed ABR represents the quotient of the respective sample relative fluorescent units (RFU) and the corresponding IgG control mix RFU. Data are expressed as the mean of RFU or ABR values from six repeated experiments, if not indicated otherwise.

Database search

The identity or characteristics of glycans was investigated by consulting the databases of the Consortium of Functional Glycomics (http://www.functionalglycomics.org/fg/) or PubMed (http://www.ncbi.nlm.nih.gov/pubmed/guide/). The online Bacterial Carbohydrate Structure Data Base (BCSDB) was consulted to identify the bacterial origin of the glycans (http://csdb.glycoscience.ru/bacterial/).

Statistical analysis

Correlation matrixes, heatmaps and hierarchical clustering were performed using “R” (The R Foundation for Statistical Computing, Version 3.0.2)[25]. Representation of the

data was done using the function heatmap.2 from the package *gplots*[26]. Hierarchical clustering and dendrograms were calculated with the complete method of the hclust function. Statistical analysis and other illustrations were performed using Microsoft Excel (Microsoft Corporation, 2011, Version 14.0.0) and GraphPad PRISM (Graphpad Software, Inc., Version 6.0c). For clique distribution analysis, only groups with common terminal carbohydrate moiety that are represented at least with 12 glycans (2% of total) on CFG glycan array version 5.1 were taken into consideration. For statistical analysis, Kruskal-Wallis, Student's *t*-test, Spearman correlation and Two-way ANOVA tests were used. Given the small size of the group (n=2), the CVID PPV^{low} subset on the NCFGv2 array was excluded when group comparisons were performed.

Further methods are available in the supplemental data, available on the *Blood* Web site.

For original data, please contact the corresponding author.

RESULTS

Broad carbohydrate reactivity defects (CRD) in diverse PAD entities

Sera from PAD patients or healthy donors (HD) were screened on CFG glycan array version 5.1 to analyze the IgG binding reactivity to 610 distinct glycans at 180μg/ml. In accordance with previous reports[9,13] this assay concentration was determined to be optimal, resulting in reproducible IgG glycan-binding patterns with minimal background. Cohorts included patients with symptomatic hypogammaglobulinemia (HGG n=76), SPAD (n=5) or IgG subclass deficiency (IgGSD; n=8), CVID (n=25), CVID with low PPV vaccination response (CVID PPV^{low}; n=6) or HD (n=43).

Using this platform, we observed broad IgG reactivity to printed glycans in pooled sera from healthy donors (Fig. 1A; Table S2), which is consistent with previously published data[9,13,21,27-29]. In contrast, marked reduction of overall glycan binding intensities was observed for all investigated PAD patient subsets, with lowest averaged relative fluorescence units (RFU) in CVID, particularly in CVID PPV^{low} patients (Fig. 1A). Next, IgG was purified from CVID, HGG and healthy donor sera by affinity chromatography, and then screened on glycan array. As with whole sera, anti-glycan reactivity of equimolar, purified IgG from immunocompromised patients presented lower RFU values on average compared to healthy controls (Fig. S1).

In an effort to compare the carbohydrate-specific IgG repertoires between PAD patients and healthy subjects, individual sera were screened. To this end glycan array version 2 from the US National Center of Functional Glycomics (NCFGv2) containing 147 glycans was used, which allowed us to include more samples. Identical glycans were similarly recognized on both arrays (Fig. S2). Figure 1B illustrates the computed reactivity matrix (mean RFU values) ordered by a dendrogram clustering algorithm[30]. Columns represent the antibody reactivity profiles

(reactivity of each specific glycan for the different sera samples), and the rows reflect the immune profiles for each patient subgroup. The dendrogrammed reactivity matrix illustrates the broader spectrum of glycan reactivity in healthy donor sera compared to all screened PAD patient subgroups, yet revealing a similar binding profile as compared to the SPAD cohort. The glycan-binding profiles of IgGSD, HGG and CVID sera displayed a narrower spectrum of glycan reactivity, which was most impaired in the CVID subgroup. CVID and CVID PPV^{low} patients also exhibited the lowest averaged RFU values (Fig. S2). No clear clustering of individual immunoprofiles was observed for total glycans, which was expected as the arrays contain synthetic glycans without known biological relevance (Fig. S2).

Glycan-specific IgG antibodies to bacterial antigens in PAD

PADs are characterized by recurrent, severe or unusual bacterial infections, especially by bacteria protected by a polysaccharide capsule. Thus, we decided to analyze the IgG reactivity profiles to known bacterial carbohydrates. On glycan array CFG version 5.1, we previously identified 121 bacterial carbohydrate antigens consulting the Bacterial Carbohydrate Structure Data Base (BCSDB)[9], providing a platform for high-throughput analysis for antibody reactivity to carbohydrate epitopes of multiple bacterial species. The printed glycans include capsular and structural oligosaccharides, as well as exopolysaccharides of commensal and pathogenic bacterial species[9]. In comparison to immunoprofiles of healthy subjects, Spearman's rank correlation analysis revealed divergent IgG reactivity profiles to bacterial glycan epitopes in PAD cohorts, with the lowest correlation of 0.34 CVID PPV^{low} patients and 0.57 for CVID, when pooled sera were screened on the CFG array (Fig. 2A). Figure 2B illustrates the collective reactivity matrix (mean RFU values) of individual sera to 65 bacterial glycans on the NCFGv2 array. Hierarchical clustering analysis revealed

a substantial loss of reactivity for the IgGSD, HGG and CVID cohorts. An extensive reduction of anti-bacterial reactivity was also found for recognition of the majority of 121 bacterial glycans on the CFG array version 5.1 in pooled sera from patients in these cohorts (Fig. S3). No clear clustering of individual immunoprofiles was observed for bacterial glycans, which may be due to differential natural exposure to bacteria (Fig. S3).

The glycan array technology combined with the consultation of the BCSDB databank allowed to screen in parallel several distinct epitopes that were identified as glycan constituents of specific bacteria. Figure 2C shows individual profiles of IgG reactivity to glycans on the NCFGv2 array that are found in *E. coli* (glycans: n=15), *H. pylori* (n=15), *N. meningitidis* (n=6), *H. influenzae* (n=3), *S. pneumoniae* (n=2), and *Salmonella* (n=2) species. Heterogenous immunoprofiles were observed in all cohorts, including healthy individuals. However, reactivity profiles were particularly low in CVID and CVID PPV^{low}, who exhibited a significant loss of IgG antibodies specific for pathogens and commensals, including antigens to which human beings are frequently exposed and immunized. Missing antibodies against Neisseria meningitis and Salmonella in the different groups may reflect lack of exposure to these pathogens.

Recognition of TACA and Siglec ligands in PAD

One life-threatening complication of PAD, in particular of CVID, is the occurrence of malignancies[1,31-34]. Since altered surface glycosylation is a hallmark of cancer and influences different aspects of tumor progression and anti-tumor immunity[7,35,36], we set out to explore IgG reactivity to tumor-associated carbohydrate antigens. Figure 3A demonstrates the IgG reactivity profiles to twenty-two glycan epitopes on CFG glycan array version 5.1 that constitute well-established TACAs. In

accordance with our previous data[9], healthy donor sera contained natural antibodies against TACAs. High reactivity was found against Lewis antigen-related TACAs, gangliosides, Thomsen-Friedenreich (TF) and globo-series-associated antigens. Loss of anti-TACA IgG reactivity was found in all examined PAD patient subgroups. The reduced binding activity by IgG was most dominant in CVID PPV^{low} donors, followed by CVID patients, as computed based on RFU profiles and represented as circular dendrogram (Fig. 3B). To further explore these findings we analyzed anti-TACA signatures of individual sera screened on the NCFGv2 array. Most sera from healthy individuals exhibited high anti–TACA reactivity to Forssman antigen, Globoside, Globo H and SSEA-4 hexaose, but heterogenous binding to other TACAs (Fig. 3C). The substantial loss of anti-TACA reactivity in CVID was confirmed in individual sera. In contrast, antibody binding to the Forssman antigen was found in all cohorts and all screened individual sera (Fig. 3A and C), indicating that this glycan-epitope is highly immunogenic with widely maintained specific antibody production in the PAD patients. Indeed, in the CVID PPV^{low} and some CVID patients, Forssman antigen was the only investigated TACA for which higher intensity signals were detected. Reactivity to GM1 was particularly low in CVID patients. This is remarkable as GM1 expression is present and positively correlates with rituximab treatment response in non-Hodgkin's lymphoma[37], which is among the most frequent malignancies occurring in these patients[10].

Overexpression of sialylated TACAs frequently occurs in tumors and hypersialylation has been linked to tumor progression and immune escape by the engagement of inhibitory Siglec receptors on leukocytes[7,36,38-40]. In PAD cohorts the antibody recognition of certain sialoglycans with known Siglec binding capacity was similar or reduced on the glycan array compared to healthy donor responses (Fig. S4). However, for two ligands of CD22/Siglec-2, expressed on B cells, binding was

high (# 377) or even increased (# 268). Little is known about the tissue expression of these two ligands and it remains to be shown if such antibodies at higher levels might interfere with the CD22 receptor / ligand axis to unleash B cell responses under certain circumstances.

Failure to raise Galα- and GalNAc-directed IgG antibodies in PAD

The composition of glycan antigens, in particular the terminal carbohydrate-moiety, has been linked to the immunogenicity of a given glycan in healthy individuals[9]. This raised the question about the effect of the relationship between immune system failure (ISF) in PAD subgroups and the structure-related immunogenicity on the architecture of the glycan-specific IgG repertoire. A binary deviation matrix was computed considering statistical deviation ($P < 0.05$) of IgG binding (RFU values) for each PAD cohort and each glycan compared to healthy donor data and reordered by a dendrogram clustering algorithm (Fig. 4A). The rows in this matrix indicate the binary antibody reactivity profiles, and the columns represent the deviation immune profiles for each PAD subgroup. By hierarchical clustering analysis four major subgroups were identified: predominant were clique 4 representing glycans with deviation in all PAD cohorts (n=293; 48%) and clique 2 containing glycans without deviation in all PAD cohorts (n=245; 40%); of lower magnitude were clique 1 (n=5; 1%) and clique 3 (n=67; 11%) encompassing glycans with heterogeneous IgG binding activities between subgroups (Table S3).

Given the association between immunogenicity and terminal carbohydrate moiety of glycans[9,41], the clique distribution of glycans was investigated based on their structure. The most dominant deviation was found for Galα- and GalNAc-terminated glycans (Fig. 4B). Forty-seven (85.5%) versus only one (1.8%) Galα-structure(s), and 37 (68.5%) versus 12 (22.2%) GalNAc-terminated glycans were

represented in clique 4 or clique 2, respectively. In accordance, the IgG antibody-binding levels (RFU values) of Galα- and GalNAc-terminated glycans were lower in all cohorts (Fig. 4C, D). In depth analysis computing a deviation matrix based on *P* values and hierarchical clustering analysis revealed large glycan clusters that were concomitantly either non-aberrant (clique B) or aberrant (clique E) for all disease entities compared to healthy individuals (Fig. 4E), whereby Galα- (70.9%) and GalNAc- (62.9%) terminated glycans were most prevalent in clique E (Fig. 4F), indicating failed antibody responses to these specific structures.

As a consequence of the inactivation of the *GGTA1* gene encoding for α1,3galactosyltransferase (GalT), humans, apes and Old World monkeys do not express the Galili epitope Galα1-3Galβ1-4GlcNAcβ[39]. Natural antibodies to this xenoantigen in most humans, eventually generated in response to the microbiota of the host, are considered a key factor in the rejection of xenografts[43], and necessitated the development of GalT knockout (GalTKO) animals[44,45]. Using a suspension array, we examined individual sera from patients (HGG, n=37; CVID, n=15; IgGSD, n=8) and healthy donors (n=18) for IgG reactivity to the Galili epitope and other Galα- and GalNAc-terminated structures including, αLN (Galα1-4GlcNAcβ), Aα3GN (Galα1-3GlcNAcβ), or A and B blood group antigens (Fig. 5A and S5). Low isohemagglutinins are frequently observed in CVID patients[11]. Consistent with this observation, we found reduced IgG reactivity to blood group A and B antigens also in the HGG, SPAD and IgGSD cohorts (Fig. S6). The IgG reactivity to Galα- and GalNAc-terminated epitopes was consistently lower in most PAD patients, whereby the reduction was most significant for the Galili epitope, as evidenced by statistical analysis (Fig. 5A and S5).

Given the significant loss of anti-Galili reactivity in PAD patients, functional implications were tested in a xenoreactivity assay, analyzing antibody-dependent cell cytotoxicity (ADCC) of primary human natural killer (NK) cells directed against the porcine kidney cell line PK15. On this cell line the Galili epitope is highly expressed on the surface and lost following enzymatic digestion by α-galactosidase as assessed by flow cytometry (Fig. 5B). Sera from healthy donors induced substantial NK cell-mediated ADCC activity against the Galili-positive PK15 cells, which was abolished following α-galactosidase treatment of the porcine target cells (Fig. 5C), illustrating the dependence of the xenogeneic activity on Gal-α epitopes, including Galili. In contrast, CVID sera failed to promote NK cell-mediated ADCC against the porcine Galili-positive target cells at equimolar IgG concentrations (1mg/mL), indicating a repertoire defect for the recognition of xenogeneic antigens. Moreover, the loss of the xenogeneic potential of CVID sera was demonstrated in a modified version of an established model for antibody-mediated skin damage[46,47], involving cryosections of porcine skin incubated with patients' sera and leukocytes from healthy donors and the assessment of dermal-epidermal separation. Porcine skin damage was significantly lower in the presence of CVID sera compared to human control sera at equimolar IgG concentrations (Fig. 5D). Together, these data provide evidence for humoral immune system failure beyond quantitative antibody deficiency, which involves repertoire defects in PAD.

DISCUSSION

The emerging picture is that the human IgG anti-carbohydrate repertoires in health[9], and in primary antibody deficiencies, exhibit a modular organization, yet with a different architecture in PAD. Translated to Cohen's concept of immune computation[48], our data imply that primary antibody deficiency is not solely characterized by aberrant antibody production, but features disturbed immune-system response states (the output) due to an altered algorithm to compute immunogenic states (the input) that is dictated by impaired cellular and molecular networks of innate and adaptive immunity[49,50].

Despite the heterogeneous genetic basis across PAD entities[1], deviation mapping revealed significant repertoire similarities pointing toward a common disease-modifying algorithm that drives humoral immune system failure. Dominant was the reduced or lost specificity for Gal$\alpha-$ or GalNAc-terminated glycan epitopes in PAD patients, for which healthy individuals express high levels of naturally occurring antibodies, eventually in response to immune stimulation by carbohydrate antigens of their microbiota[9,41]. The loss of Gal$\alpha-$ or GalNAc-specific antibodies might thus reflect the lost capacity to induce these antibodies in response to the host microbiota, or reflect the microbial dysbiosis in PAD[4], or both. Interestingly, bacteria and tumor cells use certain glycosylation patterns to escape immunity, such as sialoglycans that engage inhibitory Siglec receptors on leukocyte subsets of myeloid and lymphoid lineages[6,35,39,40,51]. It remains to be shown if naturally-occurring antibodies to TACA are also induced by the microbiota and if the observed loss has consequences for PAD patients. Notably, the loss of IgG reactivity to tumor antigens was most evident in the CVID cohort, a disorder in which the incidence of malignancy is increased[10], supporting the concept of aberrant immune surveillance in PID[52]. For instance, we

observed low antibody reactivity to TACAs known to be expressed on CVID-associated malignancies, such as GM1 in non-Hodgkin's lymphoma[37], or Thomson-Friedenreich antigen in gastric cancer[53,54]. However, tumor glycosylation patterns and their immunoreactivity remain to be fully explored for CVID-associated malignancies.

Glycoimmunology remains a relatively underdeveloped field and the need for interdisciplinary collaborations and the enhanced training of glycoscientists in biomedical areas has been identified[55]. In line with this, there is also a demand for tools, such as glycan arrays, the development of which is challenging given the availability of differently synthesized or purified glycans. However, this initial study highlights the potential and the need to expand glycan array studies in PAD using biological samples from larger patient cohorts. Clusters of glycans were identified with different reactivity profiles between PAD subgroups (cliques 3, A, C, D), which may be candidates for diagnostic use. In future studies, it will also be advisable to compare glycan-specific antibody profiles with clinical and laboratory parameters (e.g. switched memory B cell numbers, blood groups), and in specifically classified patient subsets[56].

The broad and qualitative assessment of the immune system failure (ISF) in individual patients may be informative regarding the severity of the disease, eventually leading to more personalized treatment decisions. Glycan array technology may thus provide a useful option for the individual assessment of ISF and facilitate clinical practice, especially given the heterogeneity of PAD entities with a growing list of identified pathogenetic defects[2]. However, our broad analysis demonstrates the extent of the skewed IgG repertoire with impaired reactivity to biologically relevant glycan epitopes, including those linked to PAD-associated clinical manifestations, such as infection, malignancy and autoimmunity[1,10]. Our

systems immunology approach highlights the power of high-throughput assessment of humoral immune system failure by microarray technology, which may have potential ramifications for the diagnosis, classification and therapy of PAD patients.

Acknowledgments: The authors thank Dr. Tatiana Pochechueva, Gynecology, University Hospital, Basel, for her assistance with the suspension array and Dr. Alexander Chinarev (Shemyakin Institute, Moscow) for monobiotinylated glycopolymers synthesis. We thank Dr. Yuniel Fernandez-Marrero for assistance with statistical analysis.

Funding: This work was supported in part by the Swiss National Science Foundation (grants 310030_162552 and 310030_184757) and Swiss Cancer League/Swiss Cancer Research grants KFS-3941-08-2016 and KFS-3248-08-2013 to S.V.G., and NIH/NIGMS grants P41GM103694 and GM098791 to R.D.C. H.U.S. received support from the Swiss National Science Foundation (grants No. 310030-166473 and 310030_184816) and the European Union's Horizon 2020 research and innovation program (Marie Sklodowska-Curie grant No. 642295; MEL-PLEX). The work of N.B. was supported by the Russian Scientific Foundation grant # 14-50-00131. C.J. received support from the Swiss National Science Foundation (grants No. PMPDP3_129022 and PZ00P3_161459).

AUTHORSHIP

Contributions: S.V.G. and P.J. designed the study. K.F.B., P.J. and S.V.G. wrote the manuscript. K.F.B. and S.V.G. analyzed the data. Glycan array experiments at the CFG were conducted under supervision of D.F.S. and R.D.C. Database searches

and computational analysis of the data set was performed by K.F.B. Patient sample collection, classification and preparation were done by B. G., C.J. and P.J. Experimental work was done by K.F.B., E.D.G., M.A., A.D. under supervision by D.S., H.U.S., R.R. and S.V.G. Glycan synthesis was supervised by N.B. All authors had full access to the data, helped draft the report or critically revised the draft, contributed to data interpretation, reviewed and approved the final version of the report.

Conflict-of-interest disclosure: The authors declare no competing financial interests.

***Correspondence:** Stephan von Gunten, Institute of Pharmacology, University of Bern, Inselspital INO-F, CH-3010 Bern, Switzerland; e-mail: stephan.vongunten@pki.unibe.ch

FOOTNOTES

† P.J. and K.F.B. contributed equally to this publication

REFERENCES

1. Durandy A, Kracker S, Fischer A. Primary antibody deficiencies. *Nat Rev Immunol*. 2013;13(7):519-533.

2. Bousfiha A, Jeddane L, Picard C, et al. The 2017 IUIS phenotypic classification for primary immunodeficiencies. *J Clin Immunol*. 2018;38(1):129-143.

3. Verma N, Grimbacher B, Hurst JR. Lung disease in primary antibody deficiency. *Lancet Respir Med*. 2015;3(8):651-660.

4. Berbers RM, Nierkens S, van Laar JM, Bogaert D, Leavis HL. Microbial dysbiosis in common variable immune deficiencies: evidence, causes, and consequences. *Trends Immunol*. 2017;38(3):206-216.

5. North SJ, von Gunten S, Antonopoulos A, et al. Glycomic analysis of human mast cells, eosinophils and basophils. *Glycobiology*. 2012;22(1):12-22.

6. Adams OJ, Stanczak MA, von Gunten S, Laubli H. Targeting sialic acid-Siglec interactions to reverse immune suppression in cancer. *Glycobiology*. 2017.

7. Boligan KF, Mesa C, Fernandez LE, von Gunten S. Cancer intelligence acquired (CIA): tumor glycosylation and sialylation codes dismantling antitumor defense. *Cell Mol Life Sci*. 2015;72(7):1231-1248.

8. Stowell SR, Ju T, Cummings RD. Protein glycosylation in cancer. *Annu Rev Pathol*. 2015;10:473-510.

9. Schneider C, Smith DF, Cummings RD, et al. The human IgG anti-carbohydrate repertoire exhibits a universal architecture and contains specificity for microbial attachment sites. *Sci Transl Med*. 2015;7(269):269ra261.

10. Bonilla FA, Barlan I, Chapel H, et al. International consensus document (ICON): common variable immunodeficiency disorders. *J Allergy Clin Immunol Pract*. 2016;4(1):38-59.

11. Orange JS, Ballow M, Stiehm ER, et al. Use and interpretation of diagnostic vaccination in primary immunodeficiency: a working group report of the Basic and Clinical Immunology Interest Section of the American Academy of Allergy, Asthma & Immunology. *J Allergy Clin Immunol*. 2012;130(3 Suppl):S1-24.

12. Fried AJ, Bonilla FA. Pathogenesis, diagnosis, and management of primary antibody deficiencies and infections. *Clin Microbiol Rev*. 2009;22(3):396-414.

13. von Gunten S, Smith DF, Cummings RD, et al. Intravenous immunoglobulin contains a broad repertoire of anticarbohydrate antibodies that is not restricted to the IgG2 subclass. *J Allergy Clin Immunol*. 2009;123(6):1268-1276 e1215.

14. Evans C, Bateman E, Steven R, et al. Measurement of Typhi Vi antibodies can be used to assess adaptive immunity in patients with immunodeficiency. *Clin Exp Immunol*. 2018;192(3):292-301.

15. Daly TM, Hill HR. Use and clinical interpretation of pneumococcal antibody measurements in the evaluation of humoral immune function. *Clin Vaccine Immunol*. 2015;22(2):148-152.

16. Ballow M. Vaccines in the assessment of patients for immune deficiency. *J Allergy Clin Immunol*. 2012;130(1):283-284 e285.

17. Gelfand EW, Ochs HD, Shearer WT. Controversies in IgG replacement therapy in patients with antibody deficiency diseases. *J Allergy Clin Immunol*. 2013;131(4):1001-1005.

18. Perez E, Bonilla FA, Orange JS, Ballow M. Specific antibody deficiency: controversies in diagnosis and management. *Front Immunol*. 2017;8:586.

19. Grader-Beck T, Boin F, von Gunten S, Smith D, Rosen A, Bochner BS. Antibodies recognising sulfated carbohydrates are prevalent in systemic sclerosis and associated with pulmonary vascular disease. *Ann Rheum Dis*. 2011;70(12):2218-2224.

20. Campbell CT, Gulley JL, Oyelaran O, Hodge JW, Schlom J, Gildersleeve JC. Humoral response to a viral glycan correlates with survival on PROSTVAC-VF. *Proc Natl Acad Sci U S A*. 2014;111(17):E1749-1758.

21. Stowell SR, Arthur CM, McBride R, et al. Microbial glycan microarrays define key features of host-microbial interactions. *Nat Chem Biol*. 2014;10(6):470-476.

22. Conley ME, Notarangelo LD, Etzioni A. Diagnostic criteria for primary immunodeficiencies. Representing PAGID (Pan-American Group for Immunodeficiency) and ESID (European Society for Immunodeficiencies). *Clin Immunol*. 1999;93(3):190-197.

23. Al-Herz W, Bousfiha A, Casanova JL, et al. Primary immunodeficiency diseases: an update on the classification from the international union of immunological societies expert committee for primary immunodeficiency. *Front Immunol*. 2011;2:54.

24. Blixt O, Head S, Mondala T, et al. Printed covalent glycan array for ligand profiling of diverse glycan binding proteins. *Proc Natl Acad Sci U S A*. 2004;101(49):17033-17038.

25. R Core Team. R: A language and environment for statistical computing. R Foundation for Statistical Computing, Vienna, Austria. URL https://www.R-project.org/ 2019.

26. Warnes GR, Bolker B, Bonebakker L, et al. gplot: Various R Programming Tools for Plotting Data. URL http://cran.r-project.org/package=gplots 2015.

27. Padler-Karavani V, Yu H, Cao H, et al. Diversity in specificity, abundance, and composition of anti-Neu5Gc antibodies in normal humans: potential implications for disease. *Glycobiology*. 2008;18(10):818-830.

28. Pashov A, Monzavi-Karbassi B, Kieber-Emmons T. Immune surveillance and immunotherapy: lessons from carbohydrate mimotopes. *Vaccine*. 2009;27(25-26):3405-3415.

29. Huflejt ME, Vuskovic M, Vasiliu D, et al. Anti-carbohydrate antibodies of normal sera: findings, surprises and challenges. *Mol Immunol*. 2009;46(15):3037-3049.

30. Madi A, Hecht I, Bransburg-Zabary S, et al. Organization of the autoantibody repertoire in healthy newborns and adults revealed by system level informatics of antigen microarray data. *Proc Natl Acad Sci U S A*. 2009;106(34):14484-14489.

31. Kinlen LJ, Webster AD, Bird AG, et al. Prospective study of cancer in patients with hypogammaglobulinaemia. *Lancet*. 1985;1(8423):263-266.

32. Chapel H, Lucas M, Lee M, et al. Common variable immunodeficiency disorders: division into distinct clinical phenotypes. *Blood*. 2008;112(2):277-286.

33. Resnick ES, Moshier EL, Godbold JH, Cunningham-Rundles C. Morbidity and mortality in common variable immune deficiency over 4 decades. *Blood*. 2012;119(7):1650-1657.

34. Vajdic CM, Mao L, van Leeuwen MT, Kirkpatrick P, Grulich AE, Riminton S. Are antibody deficiency disorders associated with a narrower range of cancers than other forms of immunodeficiency? *Blood*. 2010;116(8):1228-1234.

35. Fuster MM, Esko JD. The sweet and sour of cancer: glycans as novel therapeutic targets. *Nat Rev Cancer*. 2005;5(7):526-542.

36. Jandus C, Boligan KF, Chijioke O, et al. Interactions between Siglec-7/9 receptors and ligands influence NK cell-dependent tumor immunosurveillance. *J Clin Invest*. 2014;124(4):1810-1820.

37. zum Büschenfelde CM, Feuerstacke Y, Götze KS, et al. GM1 expression of non-Hodgkin's lymphoma determines susceptibility to rituximab treatment. *Cancer Res.* 2008;68(13):5414-22.

38. Varki A. Since there are PAMPs and DAMPs, there must be SAMPs? Glycan "self-associated molecular patterns" dampen innate immunity, but pathogens can mimic them. *Glycobiology*. 2011;21(9):1121-1124.

39. Stanczak MA, Siddiqui SS, Trefny MP, et al. Self-associated molecular patterns mediate cancer immune evasion by engaging Siglecs on T cells. *J Clin Invest*. 2018;128(11):4912-4923.

40. Haas Q, Boligan KF, Jandus C, et al. Siglec-9 regulates an effector memory $CD8^+$ T-cell subset that congregates in the melanoma tumor microenvironment. *Cancer Immunol Res.* 2019;7(5):707-718.

41. Soliman C, Yuriev E, Ramsland PA. Antibody recognition of aberrant glycosylation on the surface of cancer cells. *Curr Opin Struct Biol*. 2017;44:1-8.

42. Galili U. Natural anti-carbohydrate antibodies contributing to evolutionary survival of primates in viral epidemics? *Glycobiology*. 2016;26(11):1140-1150.

43. Griesemer A, Yamada K, Sykes M. Xenotransplantation: immunological hurdles and progress toward tolerance. *Immunol Rev*. 2014;258(1):241-258.

44. Lai L, Kolber-Simonds D, Park KW, et al. Production of alpha-1,3-galactosyltransferase knockout pigs by nuclear transfer cloning. *Science*. 2002;295(5557):1089-1092.

45. Phelps CJ, Koike C, Vaught TD, et al. Production of alpha 1,3-galactosyltransferase-deficient pigs. *Science*. 2003;299(5605):411-414.

46. Sitaru C, Kromminga A, Hashimoto T, Brocker EB, Zillikens D. Autoantibodies to type VII collagen mediate Fcgamma-dependent neutrophil activation and induce dermal-epidermal separation in cryosections of human skin. *Am J Pathol*. 2002;161(1):301-311.

47. de Graauw E, Sitaru C, Horn M, et al. Evidence for a role of eosinophils in blister formation in bullous pemphigoid. *Allergy*. 2017;72(7):1105-1113.

48. Cohen IR. Real and artificial immune systems: computing the state of the body. *Nat Rev Immunol*. 2007;7(7):569-574.

49. Rieckmann JC, Geiger R, Hornburg D, et al. Social network architecture of human immune cells unveiled by quantitative proteomics. *Nat Immunol*. 2017;18(5):583-593.

50. Cohen IR. The cognitive paradigm and the immunological homunculus. *Immunol Today*. 1992;13(12):490-494.

51. Macauley MS, Crocker PR, Paulson JC. Siglec-mediated regulation of immune cell function in disease. *Nat Rev Immunol*. 2014;14(10):653-666.

52. Mortaz E, Tabarsi P, Mansouri D, et al. Cancers related to immunodeficiencies: update and perspectives. *Front Immunol*. 2016;7:365.

53. Santos-Silva F, Fonseca A, Caffrey T, et al. Thomsen-Friedenreich antigen expression in gastric carcinomas is associated with MUC1 mucin VNTR polymorphism. *Glycobiology*. 2005;15(5):511-7.

54. Mereiter S, Polom K, Williams C, et al. The Thomsen-Friedenreich Antigen: A Highly Sensitive and Specific Predictor of Microsatellite Instability in Gastric Cancer. *J Clin Med.* 2018;7(9):256.

55. Agre P, Bertozzi C, Bissell M, et al. Training the next generation of biomedical investigators in glycosciences. *J Clin Invest*. 2016;126(2):405-408.

56. Picard C, Bobby Gaspar H, Al-Herz W, et al. International Union of Immunological Societies: 2017 primary immunodeficiency diseases committee report on inborn errors of immunity. *J Clin Immunol*. 2018;38(1):96-128.

FIGURE LEGENDS

Figure 1. Antibody repertoire profiling on CFG and NCFGv2 glycan arrays reveals broad carbohydrate recognition defects in symptomatic primary antibody deficiencies (PADs). (A) Glycan-specific binding of serum IgG screened at 180 μg/ml on CFG glycan array version 5.1 (610 glycans) depicted as relative fluorescence units (RFU). Screened sera were from cohorts with symptomatic hypogammaglobulinemia (HGG; n=76), specific antibody deficiency (SPAD; n=5), common variable immunodeficiency (CVID; n=25), CVID with low PPV vaccination response (CVID PPV^{low}; n=6), IgG subclass deficiency (IgGSD; n=8), or healthy donors (HD; n=43). Significant values are reported, Kruskal–Wallis test. **(B)** Glycan-binding reactivity matrices for individual sera (HD: n=12; SPAD: n=5; IgGSD: n=8; HGG: n=11; CVID: n=12) screened on the NCFGv2 array and computed by the dendrogram clustering algorithm as outlined in Materials and Methods. The color key and distribution histogram are depicted. Columns represent the antibody reactivity profiles (reactivity of each specific glycan for the different sera samples), and the rows reflect the immune profiles for each patient subgroup, based on the mean relative fluorescent units (RFU) values.

Figure 2. Recognition of bacterial carbohydrate epitopes in PADs. (A) Spearman's rank correlation matrix for IgG recognition of pooled sera to all 121 bacterial carbohydrate structures identified by BCSDB analysis on the CFG array. **(B,C)** Recognition of bacterial glycans by individual sera screened on the NCFGv2 array. **(B)** Dendrogrammed reactivity matrix based on the mean RFU values for all 65 glycans identified by BCSDB analysis. The color keys and distribution histograms are depicted. **(C)** Heatmap presentation of glycan-specific IgG binding to selected

epitopes from *S. pneumoniae* (n=2), *H. influenzae* (n=3), *N. meningitidis* (n=6), *E. coli* (n=15), *H. pylori* (n=15), and *Salmonella* (n=2) species.

Figure 3. Recognition of tumor-associated carbohydrates (TACAs) by glycan-specific IgG in PAD. (A, B) Recognition of TACAs by pooled serum IgG as screened on the CFG array and depicted as dendrogrammed glycan reactivity matrix based on ABR **(A)**, or as radial dendrogram based on RFU values **(B)**. **(C)** Heatmap presentation based on RFU values illustrating reactivity of individual serum IgG to TACAs as revealed by screening on the NCFGv2 array. The color keys and distribution histograms are depicted.

Figure 4. Deviant recognition of distinct terminal carbohydrate moieties and specific loss of Galα reactivity in symptomatic PAD. (A) Binary deviation map ($P < 0.05$) of IgG immunoprofiles compared to healthy controls based on two-way ANOVA and hierarchical clustering analysis with identification of cliques 1-4. The rows in this matrix indicate the binary antibody reactivity profiles, and the columns represent the deviation immune profiles for each PAD subgroup. **(B)** Terminal carbohydrate moieties of epitopes in reactivity cliques 2 (non-significant deviation) and 4 (significant deviation). Numeric occurrence is indicated in parenthesis. **(C, D)** Recognition of Galα- **(C)** or GalNAc- **(D)** epitopes within clique 4 (significant deviation). **(E)** Deviation map based on degree of significance with identification of cliques A-E. **(F)** Bubble chart displaying terminal glycan structure distribution across cliques A-E. The size key and percentage numbers indicate frequencies.

Figure 5. Diminished recognition of Galα-terminated glycan epitopes and reduced Galα-dependent xenogeneic anti-porcine reactivity of CVID and symptomatic IgGSD sera. (A) IgG antibody reactivity to Galili, αLN and Aα3GN

glycans as assessed by suspension array (multiplex immunoassay). Individual sera from healthy donors (n=18), HGG patients (n=37), CVID (n=15) and IgGSD (n=8) patients were analyzed. Box-and-whisker diagrams were created by the Tukey method. The middle line is plotted at the median and the box represents the interquartile range (difference between the 25^{th} and 75^{th} percentiles). Significant values are reported, Kruskal–Wallis test. **(B)** Reduced surface staining of anti-Galili mAb reactivity following α-galactosidase treatment of porcine PK15 cells, as assessed by flow cytometry. Representative histogram (left panel) and summary (right panel). **(C)** Antibody dependent cellular cytotoxicity (ADCC) activity of primary human NK cells against PK15 cells at E/T ratio of 10:1, in absence or presence of α-galactosidase. Significant values are reported (Student's *t*-test). **(D)** Histopathologic analysis of pig skin damage in cryosections incubated with healthy and patient sera in presence of healthy human leukocytes. Representative examples for each analyzed disease and control (PBS) are shown (left panel). The dashed lines indicate the dermal-epidermal junction. Pictures were taken with 40X magnification, scale bars 75µm. The damage induced was calculated as the dermal-epidermal separation normalized to the IgG concentration in the sera (right panel) (at least n=7). Results are representative of at least three **(C)** or seven **(D)** experiments. Significant values are reported (Kruskal–Wallis test).

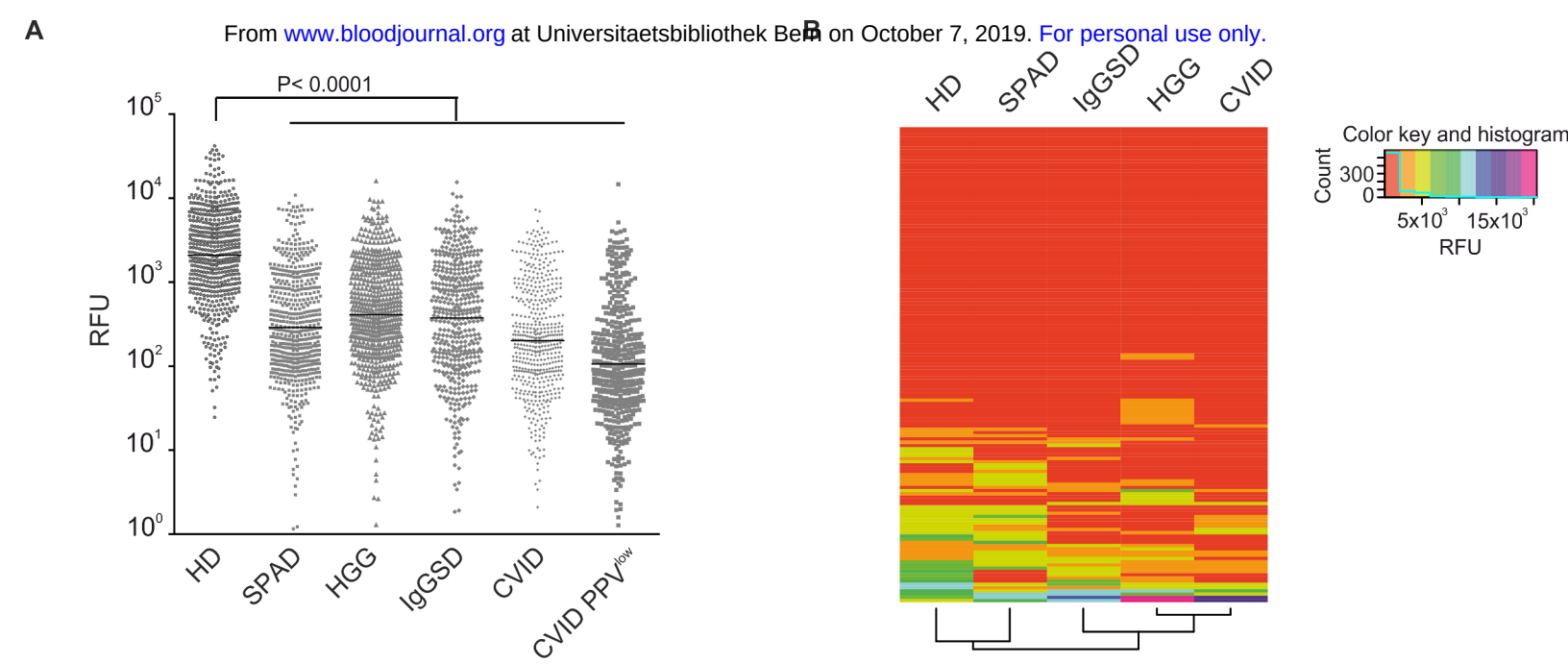

Figure1

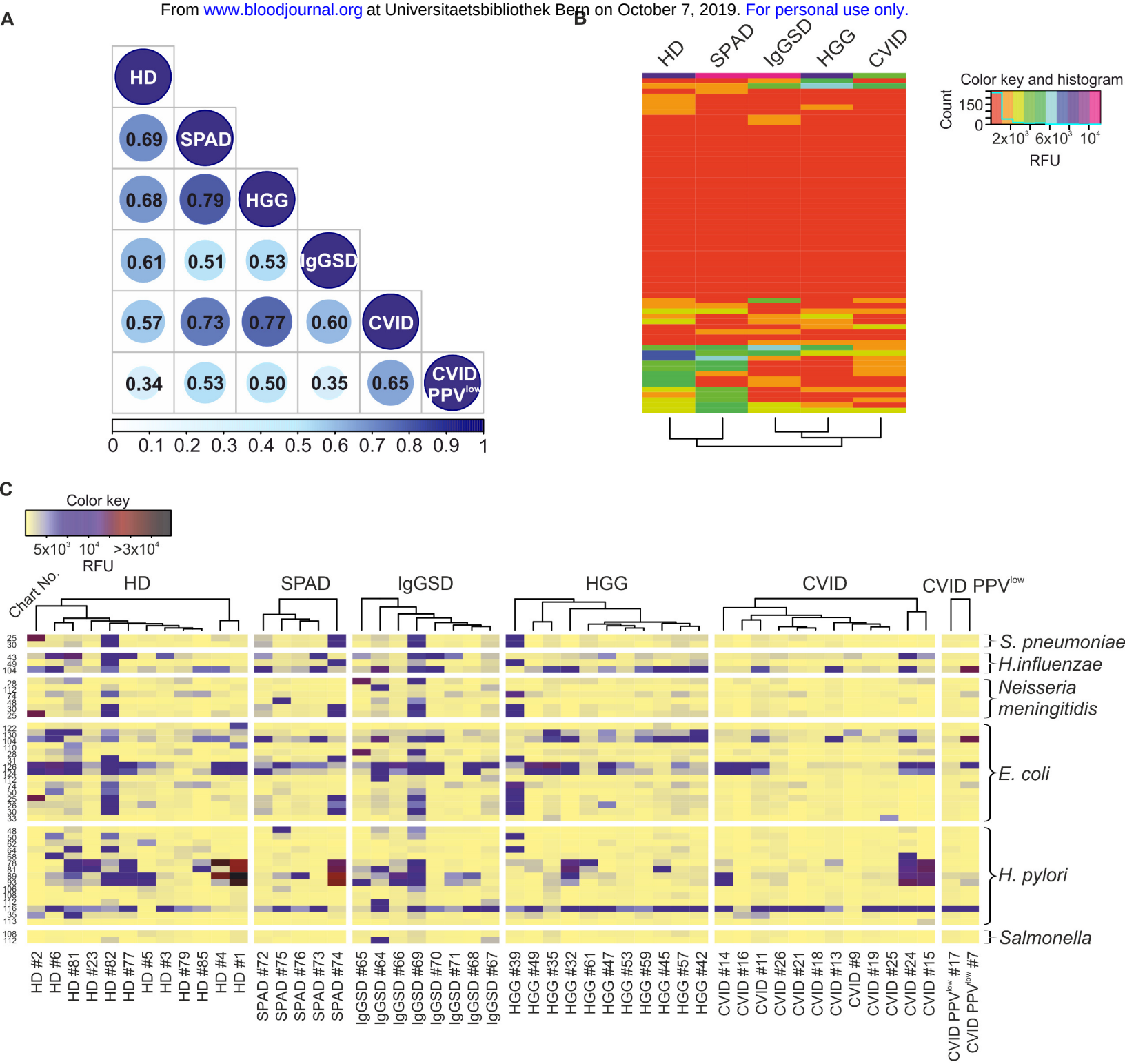

Figure 2

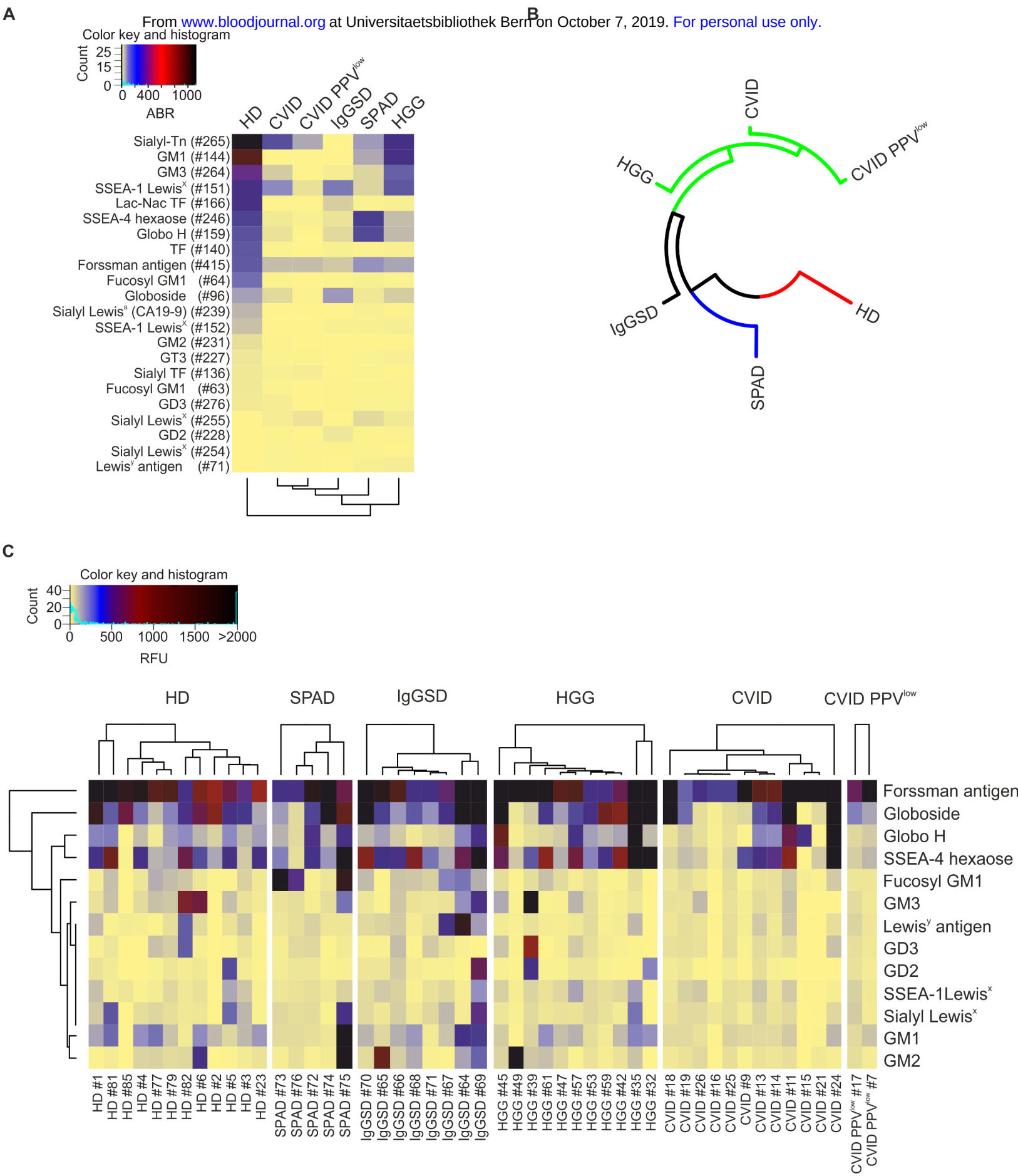

Figure 3

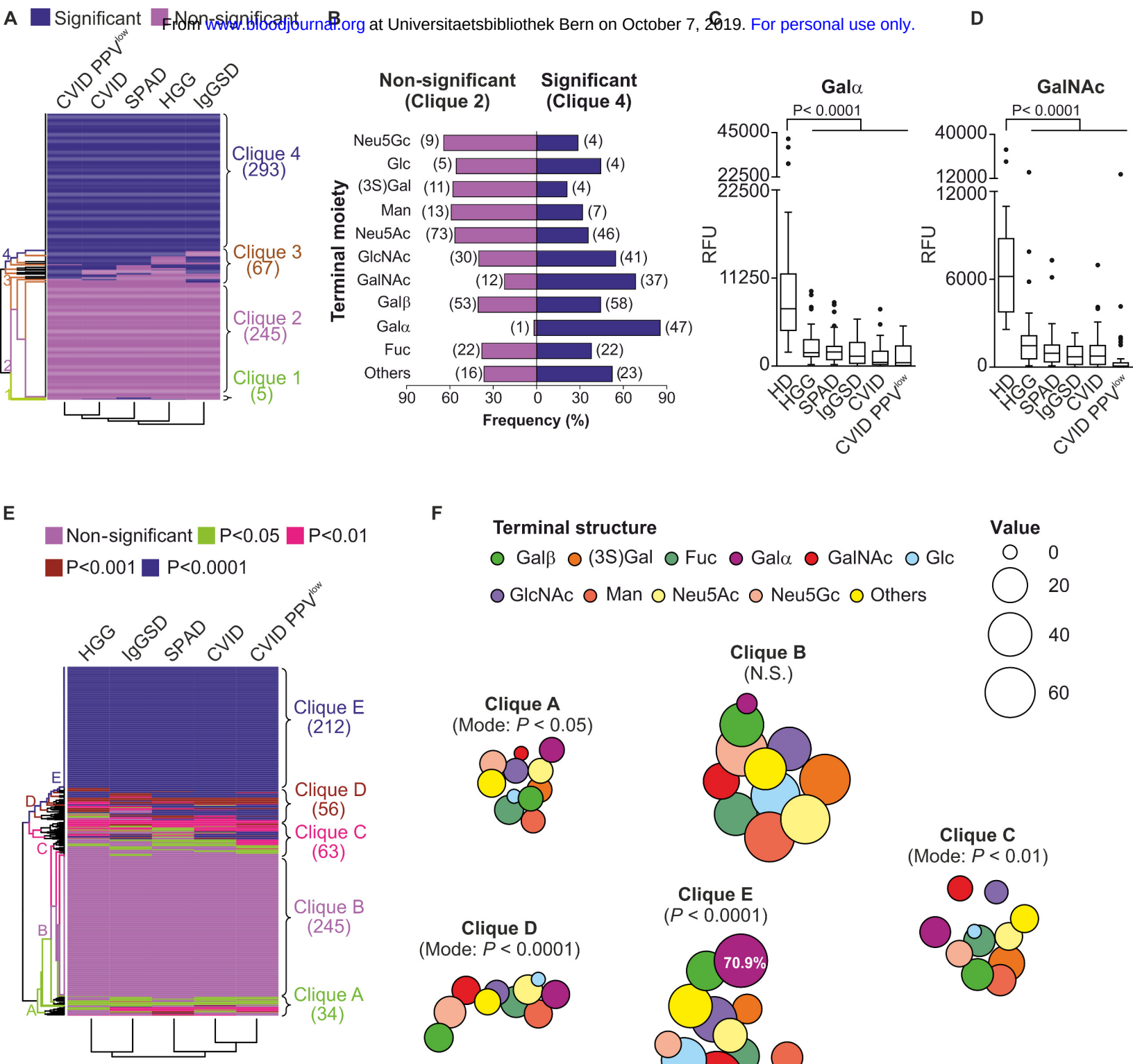

Figure 4

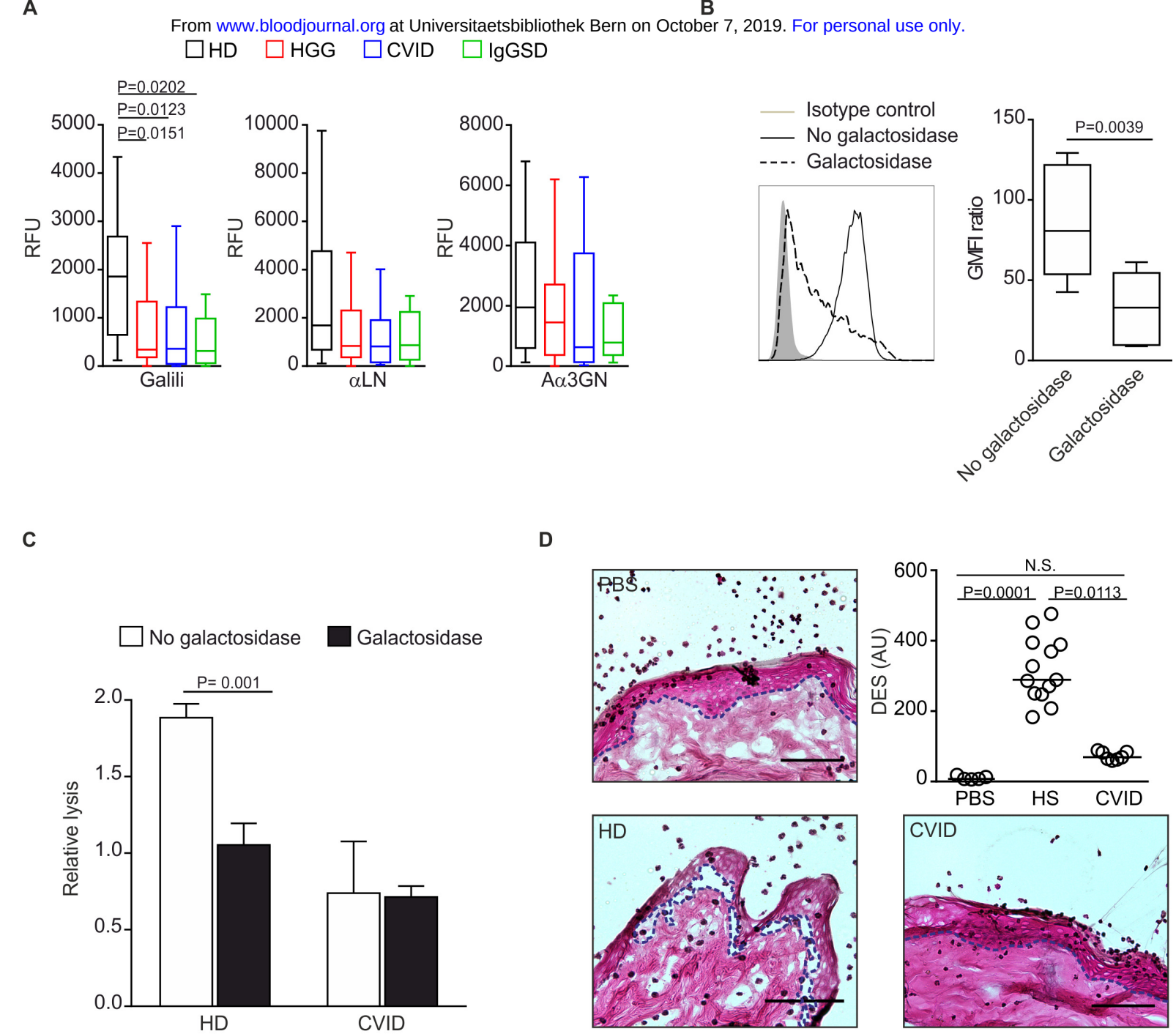

Figure 5

Prepublished online September 19, 2019;
doi:10.1182/blood.2019001705

The architecture of the IgG anti-carbohydrate repertoire in primary antibody deficiencies (PADs)

Peter Jandus, Kayluz Frias Boligan, David F. Smith, Elisabeth de Graauw, Bodo Grimbacher, Camilla Jandus, Mai M. Abdelhafez, Alain Despont, Nicolai Bovin, Dagmar Simon, Robert Rieben, Hans-Uwe Simon, Richard D. Cummings and Stephan von Gunten

Blood (print ISSN 0006-4971, online ISSN 1528-0020), is published weekly by the American Society of Hematology, 2021 L St, NW, Suite 900, Washington DC 20036.